

The characterization of strain, impurity content, and crush strength of synthetic diamond crystals

Terri L. McCormick

Department of Physics, North Carolina State University, Raleigh, North Carolina 27695-8202

W. E. Jackson

GE Superabrasives, 6325 Huntley Road, P.O. Box 568, Worthington, Ohio 43085

R. J. Nemanich

Department of Physics, North Carolina State University, Raleigh, North Carolina 27695-8202

(Received 25 July 1995; accepted 7 September 1996)

This study addresses the correlation of the macroscopic and microscopic characteristics of synthetic diamond crystals produced by high pressure, high temperature conditions. Microscopic properties were characterized using Raman spectroscopy, birefringence, and photoluminescence (PL). Macroscopic properties characterized included inclusion content and crush force. Raman measurements detected measurable stress shifts in only two samples. The PL measurements indicated an increased presence of the H3 center in areas of high strain. The absence of the H3 center and the presence of the N-V PL center was correlated to lower average crush force. A hierarchy has been developed that relates microscopic properties to average crush force.

I. INTRODUCTION

Diamonds have been synthesized using a variety of high pressure, high temperature processes. Variations of these processes lead to crystals with a large array of physical properties. Diamonds used for industrial purposes are classified by many of these process-controlled properties. Some of the industrial crystal classifications are size, shape, inclusion content, and bulk crystal strength measurements.¹ Additional physical variations observed in many industrial diamond crystals are strain and impurity content. The issue addressed herein is whether microscopic characteristics such as strain and impurity content should also be used as classification categories for diamond crystals used in industrial applications.

In this study, a series of eight different synthetic diamond samples were examined. The samples consisted of several hundred 300–500 μm average diameter synthetic diamonds grown by different high pressure high temperature processes. The samples represented typical synthetic diamonds that would be used in applications such as diamond saw tools.

Strain in diamond can result from lattice defects such as dislocations, impurities, inclusions, precipitates, cracks, and plastic deformation.² Inhomogeneous strains created by defects such as these can be observed as birefringence by illumination of the diamonds positioned between crossed polarizers. Although these strains are observable using birefringence, they are not quantifiable nor can tensile or compressive strains be distinguished. For larger strains Raman spectroscopy has been used to

measure and distinguish between tensile and compressive strains.³ Many of the previous Raman investigations of synthetic diamond have been limited to quality control and strain measurements of diamond films.³ Evans, Davey, and Robertson, however, conducted a study on synthetic diamond compacts for crystals of different grain sizes.⁴ Their results measured varying levels of strain in the compacts based on the size of the crystals. In this study, Raman spectroscopy was used to investigate areas within single synthetic diamond crystals that exhibited strain as observed through birefringence measurements.

An additional technique that can be used to study the strain in diamond is photoluminescence (PL). In previous studies of natural diamond, the broadening of the zero phonon line (ZPL) of a nitrogen impurity has been related to the inhomogeneous strain in the diamond.⁵ Additionally, comparisons of diamond compacts exhibited strain broadening of the ZPL.⁴ In this study, the broadening of the PL is used to compare the strain between the different synthetic diamond samples.

One of the primary classification schemes of natural diamond relates to the presence of nitrogen impurities. Type Ib natural diamonds are classified by the presence of large amounts of single substitutional nitrogen as opposed to aggregates and platelets detected in type Ia natural diamonds. Davies has compiled a list of known nitrogen forms, structure, and methods of detection.⁶ As in Type I natural diamond, nitrogen is the primary type of impurity in synthetic crystals. The impurity can be found in many different defect structures. Nitrogen has

been measured in both synthetic and natural diamonds by a variety of methods. Electron spin resonance (ESR), absorption, cathodoluminescence, and photoluminescence have all been utilized in detecting nitrogen in diamond. Photoluminescence has been determined to be a very sensitive method of detecting nitrogen impurities of different forms.⁷ PL has also been used for three-dimensional mapping of these impurity structures in diamond crystals.⁸ The ability to detect and map areas of impurity concentrations is beneficial in understanding the incorporation of nitrogen into the diamond. In this study PL and PL microprobe were used to detect the impurity forms and distributions. The goal was to understand the method of impurity incorporation as it related to the strain in a single crystal and to the predicted performance or measured crush strength.

II. EXPERIMENTAL

The same experimental apparatus was used for both the Raman and photoluminescence measurements. Microprobing was accomplished with a wavelength selectable argon ion laser focused through an Olympus microscope which was attached to a double spectrometer. Three different objective lenses were used for the three different investigations. The 10× objective was primarily used to observe the birefringence patterns within the diamond sample. The 50× objective was used for most of the high resolution Raman experiments due to the efficiency of light collection and a spot size of $\sim 8 \mu\text{m}$ in size. A long focal length objective with a magnification of 80× was used for studies which involved probing through the individual diamond crystals. The scattered light was collected through the same lens and then reflected into and dispersed by a U1000 ISA double spectrometer. A photomultiplier was used for detection, and a 286 AT compatible computer was used for data collection and analysis.

The Raman peak investigation involved achieving high spectral resolution measurements from selected areas of the diamond. The high resolution measurements were accomplished by using Krypton emission lines as calibration lines. The use of these lines allowed for detection of small shifts of the Raman line, and a spectral precision of $\sim 0.2 \text{ cm}^{-1}$ was achieved.

Areas of high strain were determined from examination of the birefringence pattern produced by the sample as observed in the polarizing microscope. Birefringence can be observed when a strained transparent material is placed between crossed polarizers. This technique allowed Raman and/or PL analysis of the strained areas by focusing the laser beam onto the light or dark areas of the crystals.

Both the 514.5 nm and the 457.9 nm lines of the argon ion laser were utilized to investigate the different

impurity defects within the crystal. The photon energy of the 514.5 nm line is 2.41 eV, and excitation at this energy can result in PL at energies less than the photon energy. For the 514.5 nm excitation, PL was observed in the 1.6–2.3 eV range. This line was also used for the high resolution Raman experiments. The 457.9 nm line has a photon energy of 2.71 eV, and the PL was observed in the 1.6–2.65 eV energy range. The lower cutoff in both measurements is due to the low energy cutoff of the photomultiplier tube. Raman spectra were obtained in conjunction with each PL measurement and were used to normalize the PL spectra.

PL measurements were obtained from individual single crystals and from groups of 10–20 crystals at a time. The single crystal measurements were completed using the microscope setup described for the Raman experiments. The measurements of the groups of diamond crystals were made by focusing the laser to a line image on the mounted cluster of crystals. The laser, rather than passing through the microscope, was directed onto an optical table. The beam was focused through a spherical and a cylindrical lens, and the line image had dimensions of $\sim 3 \text{ mm} \times \sim 100 \mu\text{m}$. The length and width of the focused beam allowed for sampling of several of the 300–500 μm diamonds. The crystals were mounted vertically using double sided tape in a Janis CCS-350 closed cycle refrigerator system. Spectra were obtained with the crystals at a chamber temperature of 8 K. Some heating may occur with the laser beam directed to the sample. For the samples mounted in the cryostat, the Raman scattered light was collected through a camera lens and focused into the same spectrometer system described previously.

The crush force measurements used in this analysis were determined using a roll crush system. The roll crusher makes compressive fracture strength measurements of individual grains. The system is equipped with tungsten carbide rolls, steel spring, and a linear voltage transducer. A computer records the output voltage and computes the force and statistics for entire sample sets. The crush force data used in this paper are a result of measurements from 300–500 crystals for each sample. A more complete description of the measurements and the statistics for each sample has been described previously.⁹

III. RESULTS AND DISCUSSION

A. Raman spectroscopy—Strain investigations

The Raman experiments described in this section were employed to detect strain in the crystals. Previous experiments have demonstrated that a Raman peak observed at a larger wave number shift is an indication of compressive strain while a Raman peak observed with a lesser Raman shift is indicative of tensile strain.³ Two

series of experiments were performed on the diamond samples. Experiment (A) involved the study of eight samples grown under various high pressure, high temperature conditions. Experiment (B) involved the effects of strain of the diamond from the tool-making process.

1. Samples of different growth systems

The first experiment was to measure strain differences in diamonds grown by different high pressure, high temperature processes. Several hundred diamonds of similar size, shape, and inclusion content were gathered for each set of processing conditions. The eight diamond sample sets were labeled A–H (the labeling sequence is related to the PL measurements discussed in Sec. III. B). The Raman spectra for each of these samples were obtained at several points within the crystal. Only two samples exhibited a measurable change of the Raman frequency. The Raman peaks of samples B and G were observed at 0.4 cm^{-1} and 0.5 cm^{-1} , respectively, toward higher frequencies. This is an indication of compressive strain in the samples. Using the relation for the Raman shift due to hydrostatic stress $\Delta\omega = 0.32 \text{ cm}^{-1}/\text{Kbar}$,¹⁰ these measurements correspond to a stress of 1.3 Kbar and 1.6 Kbar for samples B and G, respectively.

2. Bonding effects on strain

Raman scattering was performed to investigate the stress of diamonds that had been incorporated into tools. In order to make a saw blade or drill bit, diamonds are sintered with a bonding material such as Co. The purpose of the bond is to provide mechanical support to the diamond grains while offering the best possible adhesion to the tool blade.¹¹ The effect of this bonding material on the strain and possible performance of the tool is of interest to both the makers of the diamond and the customers that use the tools. The metal sintering process (typically $800\text{--}850 \text{ }^\circ\text{C}$ and 4000 psi) used to bond the diamond may add additional strain to the diamond. This additional strain may result in a change in performance properties differing from those anticipated by simply examining diamonds in loose unbound states. Additional strain may result in detrimental properties such as a decreased ability to bond with the material or a decrease in the amount of force or work that the diamond would normally withstand.

A comparison study was made using diamond from a single sample. The study compared the initial diamonds that had not yet been bonded, with diamonds bonded into a saw blade and diamond grit recovered from the used saw blade. Figure 1 compares these three sets of diamond. The Raman spectra indicate that no measurable increase in strain is induced into the diamond via the bonding process. Additionally, the release from the bonding material results in no change of the Raman

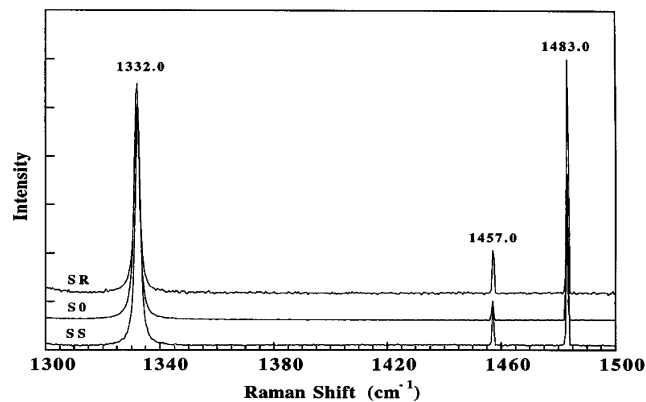


FIG. 1. Raman spectra from diamond (1332 cm^{-1}) sent through the tool formation and use process: SO represents the original diamond in grit form, SS is the diamond once it has been sintered into a blade, and SR indicates the diamond recovered after breaking free of the bond during use. An identical Raman peak frequency was observed for all three samples. The lines at 1457 and 1483 cm^{-1} are calibration lines.

spectra. These results indicate that the bonding process used to incorporate the diamond grit into saw blades induces no measurable effect on the internal strain of the diamond.

B. Photoluminescence—Impurity investigations

Sub bandgap photoluminescence occurs as a result of electron and hole recombination at a crystal defect or impurity center. These centers are termed optical centers. The optical centers studied in these diamonds have zero phonon lines (ZPL) occurring at 1.945 eV, 2.15 eV, and 2.43 eV. The centers will be referred to as the N-V center, the 2.15 eV center, and the H3 center, respectively. The optical center with a zero phonon line at 1.945 eV consists of a single substitutional nitrogen and a vacancy, in nearest neighbor positions, arranged in trigonal symmetry with the nearest neighbor carbon atom.⁴ These point defects are common to synthetic diamond and can be found dispersed throughout the crystal. The second form of impurity is the 2.15 eV ZPL, and its form is theorized to be a single nitrogen with an even (at least two) number of associated vacancies.⁴ The H3 center has a ZPL at 2.43 eV and is indicative of a vacancy trapped at a defect, called the A center. The A center consists of two nearest neighbor nitrogen atoms on C sites, and the center is not detected with PL measurements.¹² Once the A center has trapped the vacancy, the center becomes the H3 center with the vacancy in the near position between the nitrogen atoms. The H3 center is PL active, and the proposed structure has rhombic I symmetry. The H3 centers also tend to form into aggregates.¹³

Although quantitative determination of impurities is difficult with PL measurements, normalizing the PL spectra by the Raman peak allows for a semiquantitative

comparison. This technique was used here to investigate both the concentration and the distribution of the impurities within the diamonds. Four primary investigations were conducted on these samples using this technique: (i) relative concentration measurements, (ii) growth plane effects, (iii) birefringence and strain effect, and (iv) zero phonon line analysis. Through this analysis a possible model of the crystal impurity structure as it relates to the strength and strain of the diamond was constructed.

1. Impurity-defect concentration measurements

The concentration measurements were used to determine the average concentration of impurity forms from each of the samples. All measurements were obtained from (111) surfaces of the diamonds, in an unstrained area, free of inclusions. This was done in order to obtain consistency between samples. Figure 2 compares PL spectra of all of the samples obtained with the 2.41 eV excitation (514.5 nm). The spectra display the N-V center with a ZPL at 1.945 eV. The intensities of all spectra were normalized to the Raman feature for each sample. The spectra are labeled A–H as an indication of highest to lowest PL intensity from this center.

The different levels of nitrogen concentration can easily be distinguished from the spectra. Since this nitrogen impurity is found in isolated substitutional positions dispersed throughout the lattice, it is possible that the presence of this impurity in high concentrations may affect the strength of the lattice. There have been conflicting reports on this supposition. Davies suggested the possibility of a decrease in strength due to the presence of nitrogen.⁶ Hirvonen, however, reported that the implantation of nitrogen increased the strength of the diamond grit by ~30%.¹⁴ Additional reports by Bokii *et al.* suggest that a balance in the type and con-

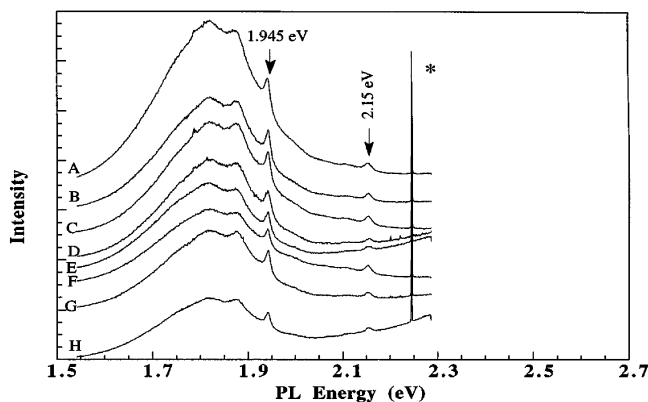


FIG. 2. PL spectra obtained with 514.5 nm (2.41 eV) excitation. The intensity of the N-V optical center, with ZPL at 1.945 eV varies for the samples. The ZPL at 2.15 eV can also be distinguished. The Raman line at $\sim 1332\text{ cm}^{-1}$ is identified by an asterisk.

centration of nitrogen impurities must be achieved to maximize the strength.¹⁵ In the experiments completed in this study, the integrated area of the PL produced by the N-V center was correlated with the average crushing force for each sample. This correlation and the calculated best linear fit is shown in Fig. 3. The correlation indicates a negative effect of N-V centers on the strength of the diamond. These results are in basic agreement with the analysis by Davies.⁶ However, as also indicated by Davies, differences in the physical properties such as metal content, morphology, aspect ratio, surface defects, and strains in the diamonds also contribute to the strength. Therefore, additional measurements of the impurities and their roles in the diamond must be investigated.

The concentration variations of the H3 center and the overall effect on the strength of the diamond were also investigated. Figure 4 illustrates the typical spectra measured for each of the samples using the 2.71 eV line (458 nm). Again, all spectra were normalized to the Raman feature. Concentration variations for the H3 center as well as the same concentration variations observed for the N-V center in Fig. 2 are seen for the samples. The trend of the data seems to indicate that the presence of H3 centers is beneficial to the strength of the diamond; however, a linear correlation was not obtained.

The inability to find a better correlation may be due to quenching effects of the H3 center signal due to the presence of other impurities. In the presence of large quantities of A-Centers (non-PL active centers), the H3 emission may be quenched by nonradiative recombination processes. Crossfield *et al.* have determined estimates that suggest that, due to a shorter decay time, the excited state may actually prefer the nonradiative decay.¹⁶ Another factor that may effect the intensity of this PL band includes the presence of nickel. It

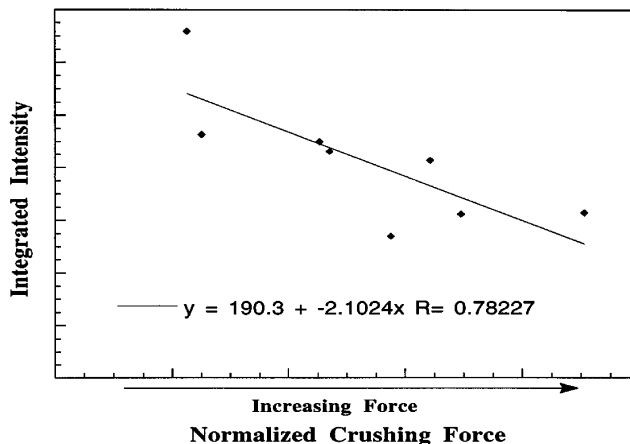


FIG. 3. Compressive strength correlation with the integrated area of the N-V center PL spectra. The graph indicates a decrease in overall strength as the nitrogen content of this form increases.

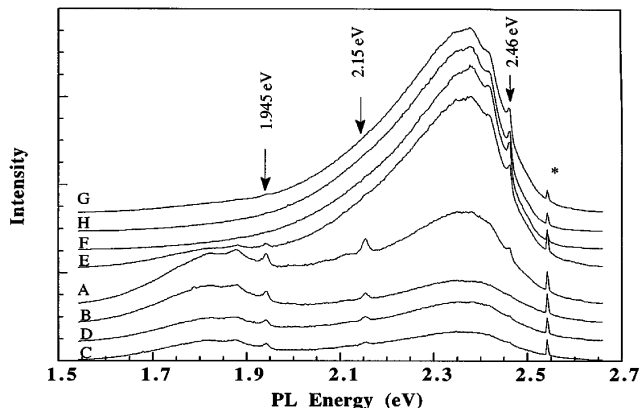


FIG. 4. PL spectra obtained with the 458 nm (2.71 eV) excitation. All three investigated optical centers are visible. The Raman line at $\sim 1332 \text{ cm}^{-1}$ is identified by an asterisk.

has been suggested that the charge compensating role of nickel helps to promote the formation of the H3 center in diamond.⁶ These possibilities complicate the PL analysis, and only distinct changes in the normalized spectra can be taken as real concentration effects. Even so, the large variations of the H3 PL signal and the trend of the greater concentrations of this impurity in the strongest diamonds should be noted.

2. Growth plane effects

As discussed earlier, each of these samples has been prepared using different growth processes; therefore, it is important to understand how the nitrogen is incorporated into the lattice and why one form may occur rather than the other. The diamonds in this study all exhibit both (111) and (100) faces, and this is a feature that classifies diamonds as cubo-octahedron.¹⁷ The incorporation of the impurities into the lattice was further examined through the study of the PL emission near the (111) and (100) growth surfaces.

Figure 5 illustrates the difference in the single substitutional nitrogen optical center (N-V) content between the (111) and (100) faces typically observed in samples A–H. This type of measurement was obtained from several diamonds of the eight original samples. The concentration of this particular center on the (111) seems to be at least double, in most cases, to that on the (100) face. This trend of higher concentration of N-V centers on the (111) face may be attributed to the trigonal shape of the impurity. The trigonal form would result from the carbon, nitrogen, and vacancy at an angle of 120° .⁸ This shape or symmetry for the nitrogen and a nearest neighbor vacancy allows for an easier incorporation on the (111) surface. Another possible explanation is the availability of more lattice sites on this face of the diamond. Due to a 15% higher density of lattice sites on the (111) face, there are more

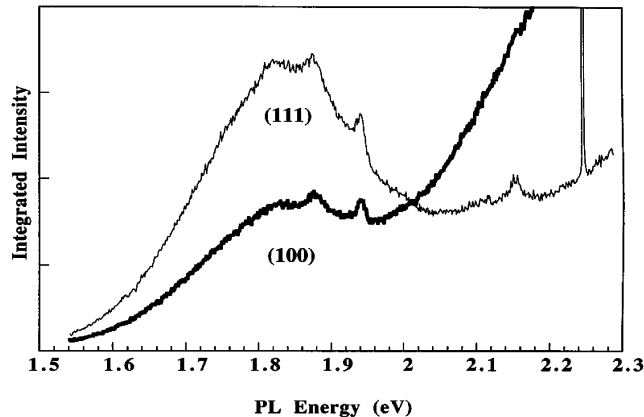


FIG. 5. Typical PL spectra (obtained with 2.41 eV excitation) comparing N-V concentrations on the (111) and (100) face of a synthetic diamond.

available sites for the impurity incorporation. However, the data reveal a 30–50% increase of N-V centers on this facet. Therefore, the facet preference of this impurity is primarily attributed to the symmetry of the impurity.

A similar correlation is observed for the H3 center on the (100) surface. Whereas the N-V center is more prominent on the (111) surface, the H3 center apparently occurs in greater concentrations on the (100) surface. Figure 6 shows typical PL spectra comparing the H3 concentrations of the (111) and (100) surface. This effect is possibly due to the Rhombic I shape of the H3 center, and the preferred orientation is along the (100) direction.⁷

Figure 7 illustrates the possible N-V center (a) and H3 center (b) incorporation into the diamond lattice. The chemical tendency of the N atom on a (growth) surface would be to relax toward a threefold coordinated site. As discussed in Ref. 7, Dodge and Beard have suggested that when nitrogen atoms form next nearest pairs along the [110] directions on the (001) face, further diamond

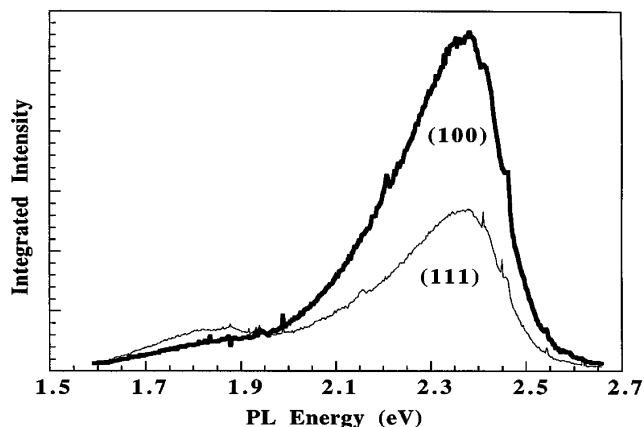


FIG. 6. Typical PL spectra (obtained with 2.71 eV excitation) comparing the H3 concentrations on the (111) and the (100) face of the diamond.

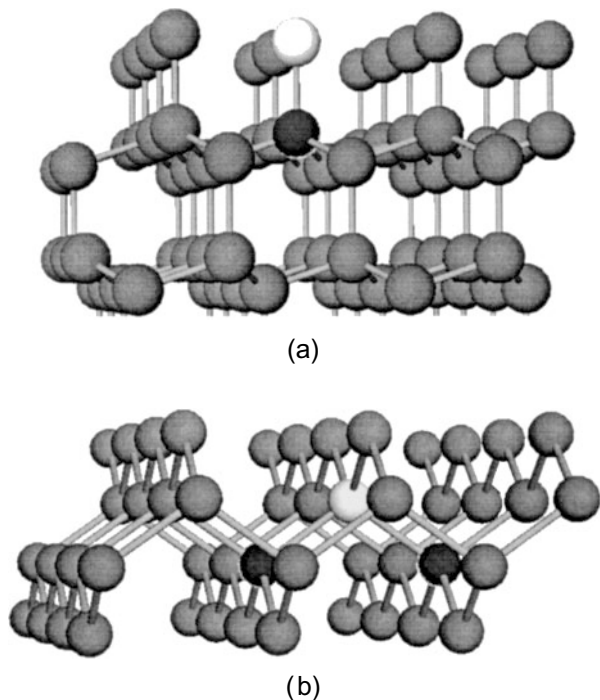


FIG. 7. Models of possible impurity incorporation into the diamond lattice: (a) N-V center incorporation into the (111) growth surface, and (b) H3 center formed on a (100) growth surface. In both cases the vacancy forms in the layer above the nitrogen impurity (or impurities).

growth envelopes the pair and may leave a vacancy at the lattice site surmounting each pair to form an N-V-N impurity arrangement. Similarly, the incorporation of a N atom in a threefold site on the (111) surface could also trap a vacancy in the next layer growth.

This detection of a high concentration of the N-V centers on the (111) surface and H3 centers on the (100) was found in all of the diamond samples. A previous experiment by Kanda and Yamaoka suggested there were two possible methods for the formation of optical centers.¹⁸ The first involved direct incorporation of the impurity into the lattice similar to that described by Dodge and Beard and discussed above. The second suggested that nitrogen in the N-V form was annealed into more complex optical centers as the diamond grew. If the second theory is correct, there should exist a high concentration of H3 or A centers in the center or internal part of the samples. The higher concentration would result from the initial or center part of the diamond, receiving longer annealing times than the final (i.e., outer) sections of growth. The spectra obtained did illustrate a slight decrease ($\sim 25\%$) in N-V centers when probing the center; however, a decrease in H3 centers was also seen. Two possible explanations could be that (i) the N-V centers were annealed into more complex centers as the diamond grew taking the form of A centers or centers not observable using PL, or (ii) the impurity concentration decreased as the diamond grew. Either

proposition has evidence to support it. The layer-by-layer growth of these crystals and the presence of H3 centers near the surface of the diamond, however, support the incorporation model by Dodge and Beard.⁷

3. Birefringence and strain effects

Birefringence is an indication of strain within a crystal and can be caused by such lattice defects as dislocations, impurities, inclusions, cracks, and plastic deformation.² Figure 8 illustrates the birefringence or strain pattern of a typical diamond found in the sample with highest crush force (*G*). This diamond, besides the small black metallic inclusions near the center of the diamond, is relatively free of inclusions. The strain patterns are observed to be emanating from the center outward toward the (111) faces of the diamond. Dislocations usually create strain emanating from the center of the crystal similar to the pattern in the picture above. Strain will also appear radiating around an inclusion or a crack.² There is no visible evidence of cracks, though some of the strain may be caused by the inclusions at the center of the diamond. Dislocations or inclusions are the most probable cause of the strain in Fig. 8. A possible indication of dislocations being the primary cause is that the strain fields radiate in a direction that is perpendicular to the primary slip planes, namely the (111) planes.

Additional evidence that some of the strain is due to dislocations was developed from the observation of the phenomenon known as trigons. These raised triangular features of the diamond are observed in the micrograph shown in Fig. 9. Trigons form at the intersection of dislocations and the surface.¹⁹ They also coincide with the (111) crystallographic plane.¹⁹ Therefore, the strain

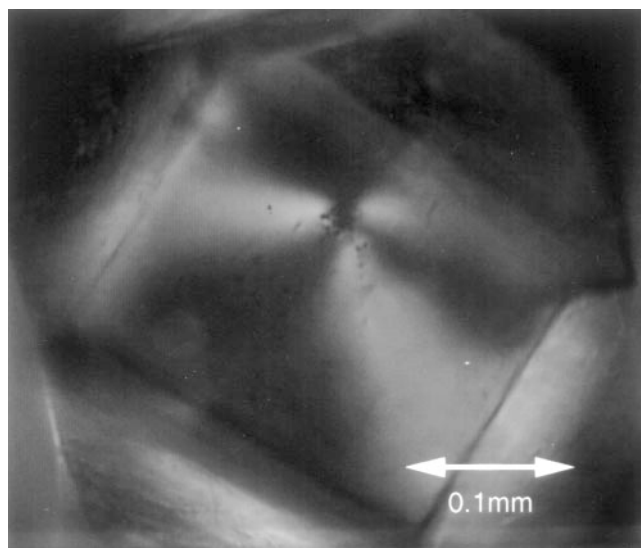


FIG. 8. Sample *G* as viewed through a 10 \times objective and crossed polarizers. The light areas indicate regions of strain. The (100) face is visible with the strain radiating out toward the (111) faces.

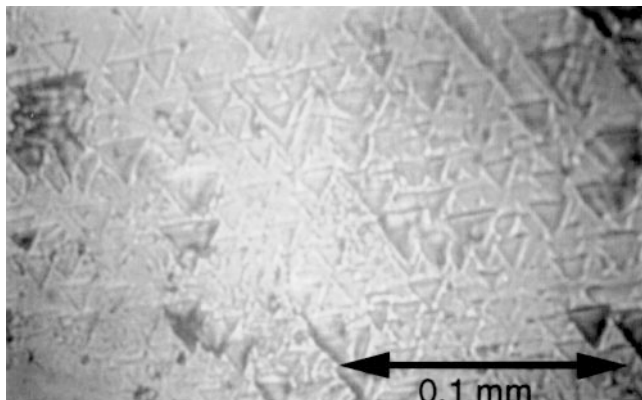


FIG. 9. Optical micrograph of a surface that displays the phenomenon called trigons. These structures have been attributed to the termination of dislocations at the surface.

observed radiating from the center of the diamond to the (111) surface in Fig. 8 could be related to dislocations if the existence of trigons can be related to the birefringence.

Wilks *et al.*¹⁹ developed a technique through which dislocations could be traced. Lines are drawn from the trigons on one face to the opposite face of the diamond. For many of the samples that they studied, these lines intersected at the center of the diamond and traced out the birefringence pattern. Thus, it is thought that, in diamonds of good quality (inclusion and crack free), the center inclusions cause dislocations that radiate from the center up the slip planes toward the (111) face. This supports the suggestion that the birefringence is due to strain around the dislocations.

The next question then is whether or not this strain distribution would have any effect on the distribution of impurities. The measurements made for this experiment concentrated on one face of individual diamond crystals. Crossed polarizers allow for the visualization of the strained areas within the diamond. The PL spectra of the dark and light areas were compared. Figure 10 shows a typical comparison of the PL spectra between the two areas. The dark areas surrounding the strain patterns were found to have higher levels of H3 and lower levels of N-V centers. The results indicate a correlation between areas of strain and the distribution of the nitrogen impurities. Spectra similar to those shown in Fig. 10 were repeatedly observed on many of the diamonds that were analyzed.

The correlation observed between impurity distribution and strain allows for a deeper insight into the properties and formation of diamond crystal. As we suggested, in the first part of this section, the strained areas radiating out from the center of the diamond most likely represent areas of dislocations. The strain produced by the dislocations can induce the clustering of nitrogen atoms, thus resulting in aggregations of the H3

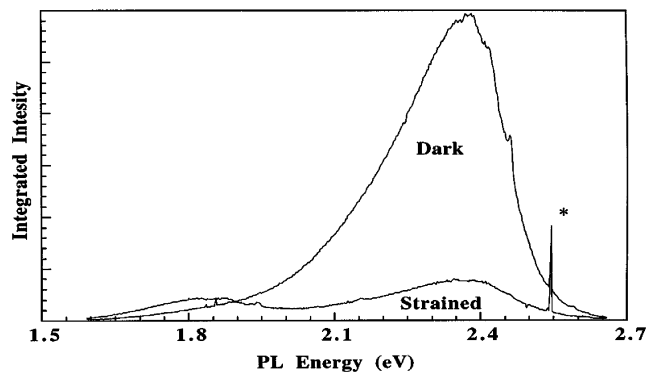


FIG. 10. PL spectra of diamond crystals showing optical birefringence indicating strain. The spectra were obtained with 2.71 eV excitation and were taken at two different positions on the same surface. The spectra taken in dark regions surrounding the strain exhibit a higher concentration of the H3 center. The Raman line at $\sim 1332 \text{ cm}^{-1}$ is identified by an asterisk.

and A centers.²⁰ Decoration of dislocations with impurity atoms is a consequence of the attraction that results between two objects with opposite strain fields.²⁰ Thus, the H3 center is not intrinsic to dislocations, rather, they aggregate around areas of dislocations as a result of the strain associated with the dislocations. Cathodoluminescence was used to detect aggregations of A centers and H3 centers surrounding areas of dislocations.²¹ This presence of these centers gathered around the dislocations indicates that the strain within the diamond is at least partially responsible for the distribution of impurities within the crystal.

Thus far, there have been two indications of dislocations derived from the results of these experiments: (i) the radiative pattern of the strain along the slip planes, and (ii) the decoration of the H3 centers around the birefringent areas of strain. A third indication of the presence of dislocations will be found in the analysis of the zero phonon lines of the PL spectra.

4. Zero phonon line measurements

The zero phonon lines of the PL spectra have been shown to be very sensitive to strain.⁴ The line shape and width are indications of the type and magnitude of the strain experienced by the impurity. When examining the ZPL at room temperature, there exists two mechanisms by which broadening occurs: (i) electron-phonon coupling at the defect and (ii) inhomogeneous strain. The first mechanism, however, is temperature dependent, and the effect becomes negligible at temperatures less than 77 K.⁴ The experiments described here were completed with the samples at $\sim 8 \text{ K}$; therefore, the second broadening mechanism is the only one of consequence. The second broadening mechanism, inhomogeneous strain, perturbs the energy levels associated with the optical centers. The broadening due to homogeneous strain or

lifetime broadening tends to be 10^3 times less than that produced by the inhomogeneous strains and are therefore negligible.

The actual line shape of the ZPL is determined by the form of defects causing the strain. Davies⁵ completed an in-depth analysis of the zero phonon lines for natural diamonds. In the analysis it was determined that a Gaussian line shape can be attributed to dislocations spatially uncorrelated throughout the lattice or to a high concentration of point defects. According to the model, randomly positioned point defects of one species, i.e., nitrogen, would result in a Lorentzian line shape.⁵ Davies concluded that most samples of diamond exhibit a line shape that is a convolution of the shape of both Lorentzian and Gaussian. He labeled this a bilorentzian. The samples in this study displayed a ZPL that varied between primarily Gaussian and up to 50% Lorentzian (bilorentzian).

The raw data of the ZPL exhibited an asymmetric line shape due to the high intensity sidebands of the luminescence. To characterize the line shape, only the high energy half of the ZPL peak was fit. Shown in Fig. 11 are the obtained fitted peaks. Here we present a symmetric line shape in which the displayed low energy half just mirrors the observed high energy half of the peak. Samples G, H, F, B, A, and C were best fit to a Gaussian, in that order (i.e., less than 10% Lorentzian component). Samples D and E were best fit with a bilorentzian, i.e., $\sim 50\%$ Lorentzian.

The line shape of these samples can thus be used to relate the distribution and location of the defects. By referring to Fig. 4, we found that four of the samples that exhibited Gaussian shaped lines were also found to have the largest concentrations of H3 centers. The birefringence observations also indicated that the four samples had the distinctive patterned birefringence radiating out from the center. Thus, the line shape is consistent with defects located around dislocations.

The other two samples, A and C, have distinguished physical properties (cracks and inclusions) and impurity concentrations that contribute to the lower strength. While Sample C as indicated from Fig. 4 exhibited a lower concentration of optical centers compared to the other samples, it may have a large density of defects that are not optically active. It is therefore proposed that the Gaussian shape from samples A and C is due to a high concentration of point defects rather than the H3 centers.

Following the line shape determination, line width and peak energy will be discussed. Even at low temperatures the ZPL are 10^3 times broader than the width caused by lifetime broadening.⁴ This broadening is apparently due to inhomogeneous strains. Figure 11 compares the ZPL for several of the samples in this experiment. Figure 12 shows the correlation between the peak energies and the FWHM of the zero phonon line.

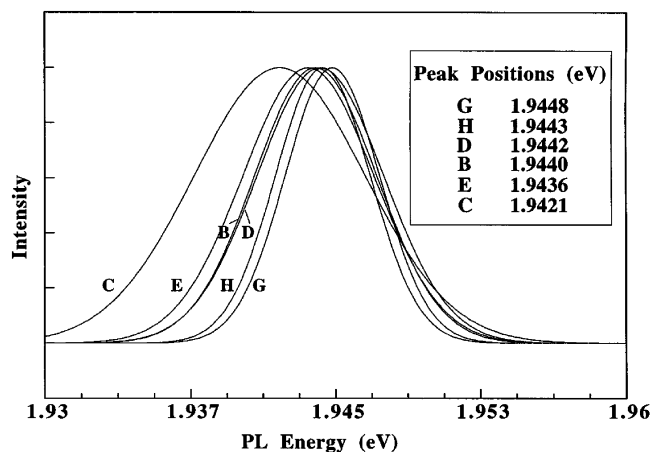


FIG. 11. Fitted zero phonon lines for six of the original eight samples. Variations in both the peak energies (given in the top right corner) and FWHM are observable.

A similar correlation was also reported by Davies.⁵ In this study of the ZPL for natural diamonds, a red shift for increasing width was observed. Again, examining samples A and C we find a distinct difference. Sample C exhibits a much higher strain broadening. Therefore, from both the FWHM and the peak position, it is found that the diamonds with the least amount of strain broadening exhibit the higher concentration of H3 centers. This is consistent with the decoration model. It was proposed in the previous section that decoration was a method of relieving strain around the dislocations.

As noted in Sec. III. A, the Raman spectra of these samples produced little if any detectable shifts. Most of the measurements were obtained at the resolution limit of the apparatus (0.2 cm^{-1}). However, a slight shift and broadening of the Raman line was observed for two of the samples. Table I shows a comparison between the FWHM of the ZPL and the FWHM and peak position of the Raman line. Using the expression for hydrostatic shift of the Raman line and the data for Sample C, we can calculate that the stress according to the Raman data should be $\sim 1.5 \text{ Kbar}$. A formula to estimate the

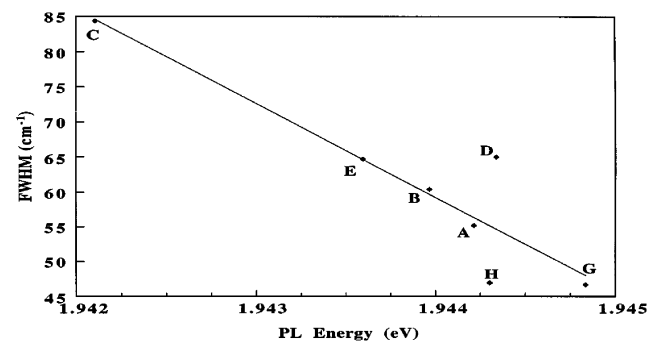


FIG. 12. Correlation of the peak energy and the FWHM of the ZPL of the diamond samples. The shift to lower energy is an indication of compressive strain fields in the region of the optical center.

TABLE I. Comparing the strain indicators in the Raman and PL spectra.

Sample	Nitrogen FWHM (cm ⁻¹)	Raman FWHM (cm ⁻¹)	Raman peak (cm ⁻¹)
H	49	2.0	1332.0
G	51	2.0	1332.0
A	56	2.0	1332.0
D	68	2.0	1332.0
B	63	2.1	1332.0
E	68	2.3	1332.0
C	89	2.3	1332.5

stress by measuring the FWHM of the 1.945 eV ZPL was introduced.⁴ The relation is

$$S = W/10, \quad (1)$$

where S is given in GPa and W is in meV. Applying this expression to the PL data results in a stress of 11 Kbar.

The ZPL calculation predicts a higher, by a factor of ten, stress within the diamond crystal. Both the PL and Raman measurements were obtained by focusing the laser onto the 10–20 diamonds at a time. The results are therefore population averages. This means that if a crystal is subjected to tensile and/or compressive strains, the shift of the Raman line will be a sum of the plus and minus shifts which could result in little or no shift. Meanwhile, the zero phonon line will broaden as a result of the sum of the absolute strains. Additionally, the PL measurements are made concerning the nitrogen environment which, as proposed previously, migrates to areas of strain. Raman measurements consider the C–C bonding throughout the entire sample volume. The existing strain may be insignificant as compared to the volume of the sample region.

The FWHM of the 1.945 eV ZPL was correlated with the strength of the diamond in Fig. 13. Other than the outlying point this correlation seems to indicate

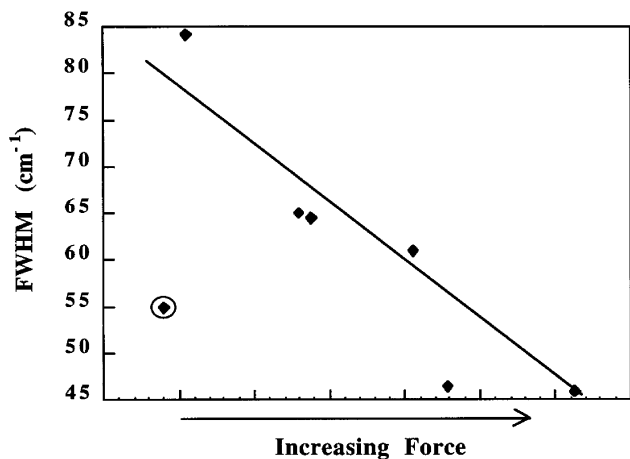


FIG. 13. Correlation of the FWHM of the 1.945 eV ZPL with the strength of the diamond grit.

that the strain which affects the optical centers is indeed related to the strength. The outlying point, however, is disturbing to this analysis, that is, until the macroscopic properties of the particular diamonds are observed. Figures 14(a) and 14(b) are optical micrographs of typical diamonds from the sample of the outlying point (sample A) and of one from another sample (sample G) with similar PL and Raman characteristics. It is apparent from the micrographs that the physical properties, i.e., fractures, cracks, shape, and inclusion content, are responsible for the low strength measurements of this sample.

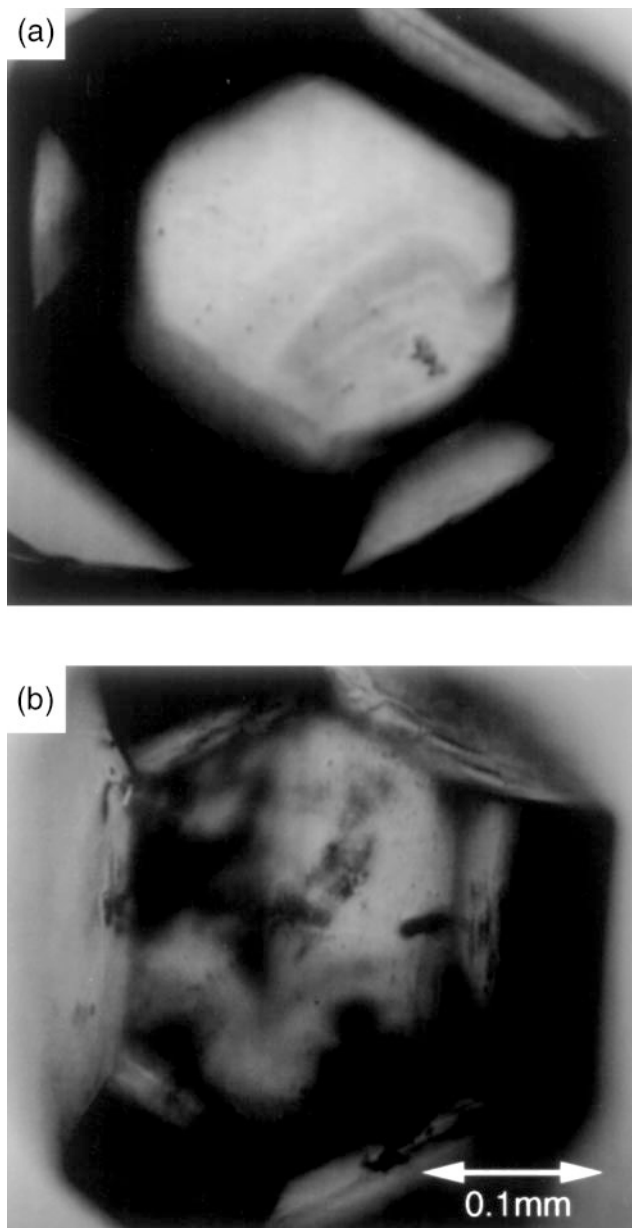


FIG. 14. Optical micrographs of diamond from two different sample groups: (a) Sample G which is relatively free of physical defects, and (b) Sample A which is filled with cracks and high levels of inclusion content.

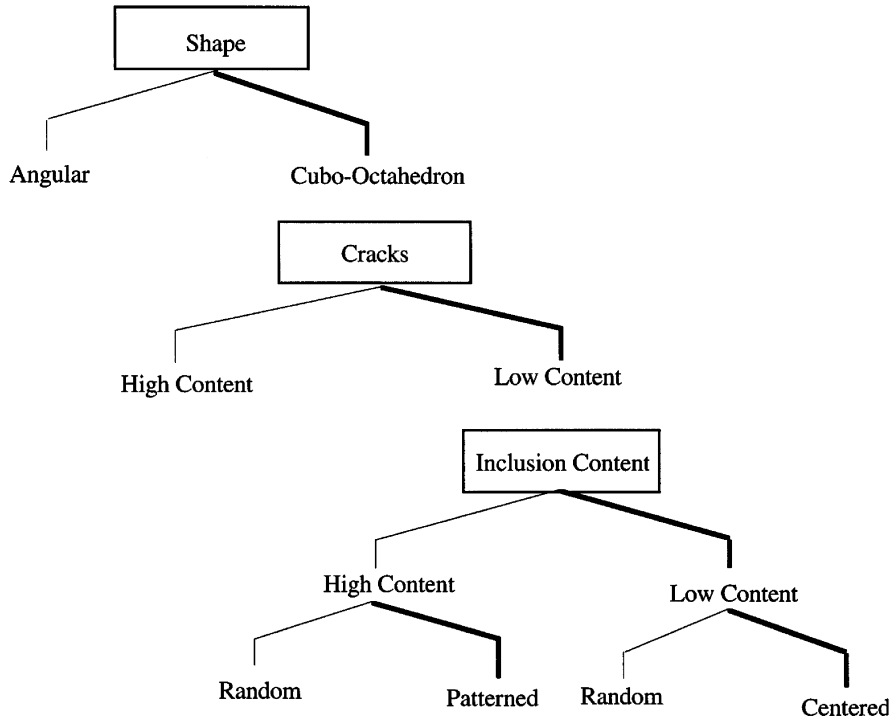


FIG. 15. Hierarchy of macroscopic physical properties as they relate to strength. The darker line represents the strongest property path.

Consider the effects of the physical properties of the samples on the strength of the diamond. The effects of cracks and fractures have long been determined to weaken the crystal.²² Inclusions have been a more recent topic in that there has been some debate over whether the metal inclusions would help strengthen the diamond by acting to stop crack propagation²³ or whether they would weaken the diamond by expanding during use and initiating a crack. Recent studies report inclusions as detrimental to the strength of the diamond.⁶ It is possible, however, that the arrangement of the inclusions may also determine which role the inclusions play. In some of the

diamonds a great deal of inclusions exists, but they are arranged in ray patterns radiating out from the center of the diamond to the outer face. The inclusion ray patterns are similar in size and direction to the birefringence rays observed in the samples with the only inclusions found in the center of the diamond. This may indicate that in some cases inclusions, like impurities on the microscale, gather in and around dislocations. In this case the inclusions may contribute to the increase in strength of the diamond by forming what is known as whiskers by filling in separated areas and acting as binding for the areas of dislocations, cracks, and fractures.

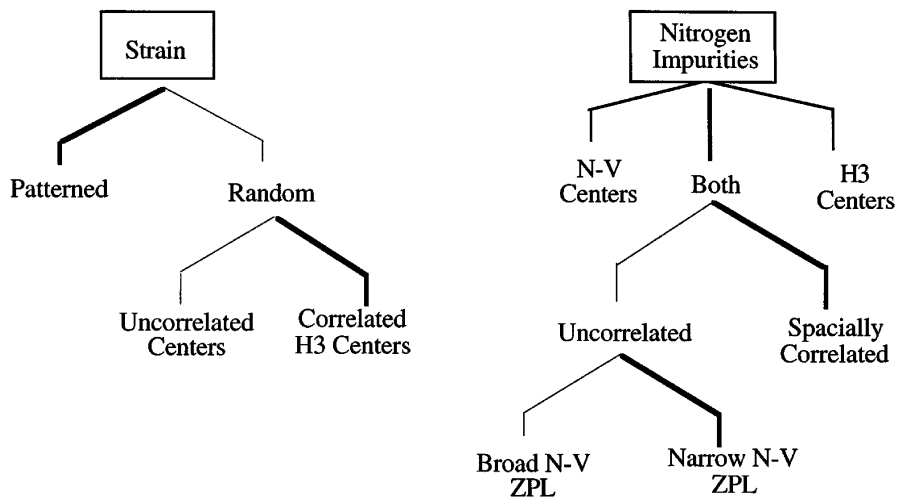


FIG. 16. Hierarchy of microscopic properties of diamond. Again, the darker line illustrates the path of the positive strength related properties.

IV. CONCLUDING REMARKS

We have determined throughout this analysis that there are many components that may affect the strength of the diamond. These qualities can be divided into two groups: macroscopic and microscopic characteristics. The macroscopic characteristics consist primarily of physical properties such as size, shape, fracture, and inclusion content. In most cases the shape is considered to be the most critical property for the strength of the diamond, followed by the presence of high concentrations of internal cracks. The inclusion content falls next in this type of strength, determining hierarchy followed by the arrangements of the inclusions. Figure 15 represents this type of hierarchy, and illustrates the macroscopic qualities that most affect the strength of the crystal.

The primary focus of this analysis, however, was to determine a microscopic hierarchy of strength-determining features. These features include strain, impurity forms, and distributions. The hierarchy derived from the experiments presented here is shown in Fig. 16, and a proposed model of the effect of these features is given below.

It appears from comparing both the microscopic properties and the macroscopic qualities a uniformity can be observed. The inclusions, impurities, and strain seem to function in a similar manner when affecting the strength of the diamond. The model proposed here correlates the function of the impurities with that of the inclusions. On a much less dramatic scale, the impurity aggregates seem to function as binding or whiskers in the dislocated areas. The aggregates would then function to pin the dislocations and microfractures within the diamond, thus resisting further fracturing or dislocation movement and strengthening the diamond. The dispersed nitrogen seems to add to the overall inhomogeneous strain throughout the crystal, thus weakening the crystal.

In summary, several features of the microscopic properties in diamond have been studied. The results indicate that the presence of nitrogen in a particular form does affect the strength of the crystal. The increased presence of the H3 center as opposed to the N-V center appears to be a strength-increasing factor. It was also determined that the distribution of these impurities throughout the diamond was not completely homogeneous. The distribution of the N-V and H3 centers were correlated with strain patterns that existed in the diamond. The more complex form (H3) was seen to aggregate around what was determined to be regions of possible dislocations. One explanation given for this aggregation effect was impurity decoration of the dislocations. Additional observations made in this analysis included the preference of the N-V center for the (111) surface and the H3 center for the (100) surface.

These preferences are attributed to the symmetry of the optical center and the growth process. Studies of the ZPL verified a similar broadening and shifting between the PL peak and the Raman line. Calculations, however, indicate a magnitude difference in the results for strain between the two measurements. A quantitative measurement for calculating the magnitude of the tensile or compressive strain using the ZPL has yet to be identified.

ACKNOWLEDGMENTS

We gratefully acknowledge many helpful discussions with Leah Bergman. The research at NCSU was supported in part through grants from GE Superabrasives and the Office of Naval Research.

REFERENCES

1. J. Wilks and E. Wilks, *Properties and Applications of Diamond* (Butterworth Heinemann, Oxford, 1991).
2. A. R. Lang, *Nature* (London), 248–251 (1967).
3. R. J. Nemanich, in *Annual Review of Material Science*, edited by R. A. Huggins, J. A. Giordmaine, and J. B. Wachtman, Jr. (1991), Vol. 21, pp. 535–558.
4. T. Evans, S. T. Davey, and S. H. Robertson, *J. Mater. Sci.* **19**, 2405–2414 (1984).
5. G. Davies, *J. Phys. C* **3**, 2474–2486 (1970).
6. G. Davies, *Chemistry and Physics of Carbon*, edited by P. L. Walker (Marcel Dekker, New York, 1982), Vol. 11, pp. 70–71.
7. C. D. Clark, in *Properties of Natural and Synthetic Diamond*, edited by J. E. Field (Academic Press, London, 1992), p. 66.
8. W. J. P. Van Enkevort and H. G. M. Lochs, *J. Appl. Phys.* **64**, 434–437 (1988).
9. S. W. Webb and W. E. Jackson, *J. Mater. Res.* **10**, 1700–1709 (1995).
10. M. H. Grimsditch, E. Anastassakis, and M. Cardona, *Phys. Rev. B* **18**, 901 (1978).
11. P. N. Tomlinson, in *The Properties of Natural and Synthetic Diamonds*, edited by J. E. Field (Academic Press, San Diego, CA, 1992), pp. 640–641.
12. A. T. Collins, *J. Phys. C* **13**, 2641–2650 (1980).
13. T. Evans, S. T. Davey, and S. H. Robertson, *J. Mater. Sci.* **19**, 2405–2414 (1984).
14. J. K. Hirvonen, *J. Metals* **39** (11), 58–60 (1987).
15. G. B. Bokii, N. F. Kirova, and V. I. Nepsha, *Sov. Phys. Dokl.* **24**, 83–84 (1979).
16. M. D. Crossfield, G. Davies, A. T. Collins, and E. C. Lightowers, *J. Phys. C* **7**, 1909–1917 (1974).
17. R. C. Burns and G. J. Davies, in *The Properties of Natural and Synthetic Diamond*, edited by J. E. Field (Academic Press Inc., San Diego, CA, 1992), p. 412.
18. H. Kanda and S. Yamaoka, *Diamond and Relat. Mater.* **2**, 1420–1423 (1993).
19. E. M. Wilks and J. Wilks, *Industrial Diamond Review* **31**, 238–243 (1971).
20. W. J. P. Van Enkevort and E. P. Visser, *Philos. Mag. B* **62**, 597–614 (1990).
21. R. J. Graham and K. V. Ravi, *Appl. Phys. Lett.* **60**, 1310–1312 (1992).
22. J. Wilks, *Industrial Diamond Review* **33**, 382–390 (1973).
23. L. Bergman, private communication.